ELSEVIER

Fuel Vol. 75 No. 3, pp. 289–294, 1996

0016-2361/96/$15.00 + 0.00

0016-2361(95)00269-3

The P-1 model for thermal radiation transfer: advantages and limitations

S. S. Sazhin, E. M. Sazhina, O. Faltsi-Saravelou and P. Wild
Fluent Europe Ltd, Holmwood House, Cortworth Road, Sheffield S11 9LP, UK
(Received 10 February 1995; revised 26 September 1995)

The P-1 model for thermal radiation transfer is re-examined in view of its potential applications to industrial problems as part of a computational fluid dynamics (CFD) analysis. The concept of radiation temperature adopted is shown to be particularly useful when this model is used in a general curvilinear coordinate system. An explanation is given as to why the P-1 model gives reliable predictions in the case of 1D plane geometry in both optically thin and optically thick media, while it overestimates the radiation heat fluxes from localized heat sources in optically thin media. It is pointed out that the P-1 model is particularly useful for accounting for the radiative exchange between gas and particles. The results of modelling of coal combustion processes in an industrial furnace based on the P-1 model are shown to be consistent with experimental observations.

(Keywords: radiative heat transfer; mathematical modelling; coal combustion)

In the majority of industrial combustion devices, thermal radiation is the dominant mode of energy transfer. The quantitative modelling of these devices therefore relies on an accurate and computationally efficient thermal radiation transfer model to predict flame shape and temperature correctly. The accurate prediction of pollutants such as nitrogen oxides also relies on proper treatment of thermal radiation transfer.

Different models of thermal radiation transfer have been discussed in many papers (see e.g. ref. 1). It is not the intention here to review this subject. Instead the focus is on some practical aspects of the application of one of these models, the P-1 model: its advantages and limitations. It is thought that this will be particularly useful for engineers dealing with practical modelling of fuel combustion processes.

The general equation of transfer for the variation of intensity of thermal radiation at position $\boldsymbol{r}$ along the s-direction (in the direction of the unit vector $\boldsymbol{s}$) can be written[1] as

$$\frac{\mathrm{d}i'_\lambda}{\mathrm{d}s} = a_\lambda i'_{\lambda\mathrm{b}} - (a_\lambda + \sigma_{\mathrm{s}\lambda}) i'_\lambda + \frac{\sigma_{\mathrm{s}\lambda}}{4\pi} \int_{\omega_i=0}^{4\pi} i'_\lambda(s, \omega_i)\Phi(\lambda, \omega, \omega_i)\,\mathrm{d}\omega_i \tag{1}$$

where $i'_\lambda = i'_\lambda(\lambda, s, \omega)$ is the spectral intensity of radiation in the unit solid angle ω, a_λ is the absorption coefficient depending on the wavelength λ, $\sigma_{\mathrm{s}\lambda}$ is the scattering coefficient, $\Phi(\lambda, \omega, \omega_i)$ is the phase function of scattering, and $i'_{\lambda\mathrm{b}} = i'_{\lambda\mathrm{b}}(\lambda, s, \omega)$ is the spectral density of the radiation of the medium.

In a grey medium with uniform a_λ and $\sigma_{\mathrm{s}\lambda}$ and $\Phi(\lambda. \omega, \omega_i) = 1$, Equation (1) can be integrated over λ to give

$$\sum_{i=1}^{3} l_i \frac{\partial i'}{\partial \kappa_i} + i' = (1 - \Omega) i'_\mathrm{b} + \frac{\Omega}{4\pi} \int_{\omega_i=0}^{4\pi} i'(s, \omega_i)\,\mathrm{d}\omega_i \tag{2}$$

where $l_1 = \cos\theta, l_2 = \sin\theta\cos\varphi \equiv \cos\delta, l_3 = \sin\theta\sin\varphi \equiv \cos\gamma$ are directional cosines of the vector $\boldsymbol{i}'$, $\kappa_i = (a + \sigma_s)x_i$, and $\Omega = \sigma_\mathrm{s}/(a + \sigma_\mathrm{s})$.

The complexity of Equations (1) and (2) lies in the fact that the radiation intensity i_λ is a function not only of the position $\boldsymbol{r}$ but also of the direction of $\boldsymbol{s}$. Hence the computation of i' requires discretization not only in space (essential for any computational fluid dynamics (CFD) problem) but also in the directions of the radiation propagation. The way in which the latter discretization is performed determines different radiation transfer models. Unfortunately, for the moment there is no universally accepted radiation transfer model that could be applied to all industrial problems, and the choice of the model is often based on engineers' experience and intuition.

A detailed comparison between different models of thermal radiation transfer has been made in a number of review papers and monographs (see e.g. refs 1, 2). This paper concentrates on only one of these models, which uses a particular way of discretization of i' with respect to angles θ and φ: the P-1 model (see ref. 1).

Basic equations of the P-1 model and the approximations used are discussed first. A qualitative analysis of the limitations of the P-1 model is then given, followed by the generalization of the P-1 model so that the effects of radiative exchange between gas and particles can be accounted for. Finally, the application of the P-1 model to coal combustion in a real furnace is demonstrated.

THEORY

The P-1 model is the simplest case of the more general P-N model. The latter is based on the expansion of i' in an orthogonal series of spherical harmonics:

$$i'(s,\omega) = \sum_{l=0}^{\infty}\sum_{m=-l}^{l} A_l^m(s) Y_l^m(\omega) \tag{3}$$

where $A_l^m(s)$ are coefficients to be determined by the solution and $Y_l^m(\omega)$ are angularly dependent normalized spherical harmonics given by

$$Y_l^m(\omega) = \left[\frac{2l+1}{4\pi}\frac{(l-m)!}{(l+m)!}\right]^{1/2} \mathrm{e}^{im\varphi} P_l^m(\cos\theta) \tag{4}$$

where $P_l^m(\cos\theta)$ are associated Legendre polynomials of the first kind, defined as

$$P_l^m(\mu) = \frac{(1-\mu^2)^{m/2}}{2^l l!}\frac{\mathrm{d}^{l+m}}{\mathrm{d}\mu^{l+m}}(\mu^2-1)^l \tag{5}$$

In the limit $l \to \infty$, the approximation (3) is exact. However, the computational requirements appear to be unrealistically high when l is > 5, and these values have practically never been used. In many practically important problems, especially in an optically thick medium, it appears sufficient to restrict the summation (3) by $l = 0$ and $l = 1$. In this case the P-N model is known as the P-1 model. Expression (3) for the P-1 model can be simplified to

$$i'(s,\theta,\varphi) = \frac{1}{4\pi}(i'^{(0)} + 3i'^{(1)}\cos\theta + 3i'^{(2)}\sin\theta\cos\varphi + 3i'^{(3)}\sin\theta\sin\varphi) \tag{6}$$

where:

$$i'^{(0)} \equiv i'^{(0)}(s) = \int_{\omega=0}^{4\pi} i'(s,\omega)\,\mathrm{d}\omega \tag{7}$$

$$i'^{(i)} \equiv i'^{(i)}(s) = \int_{\omega=0}^{4\pi} l_i i'(s,\omega)\,\mathrm{d}\omega \tag{8}$$

In view of Equation (7), Equation (2) can be written in a simplified form:

$$\sum_{i=1}^{3} l_i\frac{\partial i'}{\partial\kappa_i} + i' = (1-\Omega)i'_{\mathrm{b}} + \frac{\Omega}{4\pi}i'^{(0)} \tag{9}$$

From Equation (9), moment equations can be generated by multiplying it by 1 and l_j and integrating over all solid angles. Hence

$$\sum_{i=1}^{3}\frac{\partial i'^{(i)}}{\partial\kappa_i} = (1-\Omega)(4\pi i'_{\mathrm{b}} - i'^{(0)}) \tag{10}$$

$$\sum_{i=1}^{3}\frac{\partial i'^{(ij)}}{\partial\kappa_i} = -i'^{(j)} \tag{11}$$

where

$$i'^{(ij)} = \int_{\omega=0}^{4\pi} l_i l_j i'(s,\omega)\,\mathrm{d}\omega \tag{12}$$

Substituting Equation (6) into Equation (12) gives

$$i'^{(ij)} = \frac{1}{3}\delta_{ij} i'^{(0)}(s,\omega) \tag{13}$$

Substituting Equation (13) into Equation (11) yields the final set of four equations for the four unknown parameters $i'^{(0)}$ and $i'^{(i)}$ $(i = 1, 2, 3)$:

$$\left.\begin{aligned} \sum_{i=1}^{3}\frac{\partial i'^{(i)}}{\partial\kappa_i} &= (1-\Omega)(4\pi i'_{\mathrm{b}} - i'^{(0)}) \\ \frac{\partial i'^{(0)}}{\partial\kappa_i} &= -3i'^{(i)} \end{aligned}\right\} \tag{14}$$

However, the system of equations (14) can be further simplified before it is used for numerical computations. To start with, following e.g. ref. 3, the radiation temperature is introduced as:

$$\theta_{\mathrm{R}}^4 = \frac{i'^{(0)}}{4\sigma} \tag{15}$$

by analogy with the conventional temperature T, for which $4\pi i'_{\mathrm{b}} = 4\sigma T^4$.

Also, based on Equation (8), the radiation flux $\boldsymbol{q}$ with the components $q_i = i'^{(i)}$ can be introduced. In view of Equation (15), the last three equations in the system (14) can be reduced to

$$\boldsymbol{q} = -\frac{4\sigma}{3(a+\sigma_s)}\boldsymbol{\nabla}\theta_{\mathrm{R}}^4 \tag{16}$$

Taking divergence of both sides of Equation (16) gives

$$\boldsymbol{\nabla q} = -\boldsymbol{\nabla}\frac{4\sigma}{3(a+\sigma_s)}\boldsymbol{\nabla}\theta_{\mathrm{R}}^4 \tag{17}$$

The expression $-\boldsymbol{\nabla q}$ can be directly substituted into the enthalpy equation to account for the radiation transfer process, provided that the distribution of θ_{R} is known. As a zeroth approximation it may be assumed that $\theta_{\mathrm{R}} = T$ (Rosseland approximation) and in this case the effect of radiation can be accounted for by simple correction of the thermal conductivity and introducing the slip boundary conditions (see ref. 1 pp. 836–837). This approximation, being reasonably good for an optically thick medium, can give misleading results when $a + \sigma_{\mathrm{s}}$ is not sufficiently large. A better approximation can be obtained if Equation (17) is substituted into the first equation of the system (14). As a result, the equation for θ_{R} is obtained in the form

$$\frac{1}{3a}\boldsymbol{\nabla}\frac{1}{a+s_{\mathrm{s}}}\boldsymbol{\nabla}\theta_{\mathrm{R}}^4 - \theta_{\mathrm{R}}^4 + T^4 = 0 \tag{18}$$

In the absence of scattering and for cylindrical geometry, this equation reduces to that derived in ref. 4.

The boundary conditions for Equation (18) are determined by the following equations. First, the incident flux on the boundary, q_{inc}, can be determined by the equation (see Equation (7.20b) in ref. 1)

$$q_{\mathrm{inc}} = \sigma T_\omega^4 - \frac{q_{\mathrm{n}}(0)}{\epsilon_\omega} \tag{19}$$

where T_ω is the wall temperature, $q_n(0)$ is the normal component of the vector $\boldsymbol{q}$ defined by Equation (16), ϵ_ω is the emissivity of the wall, and the argument $s = 0$ refers to the boundary.

On the other hand, from Marshak boundary conditions[5] it follows that (cf. Equation (15–132) of ref. 1)

$$q_{\mathrm{inc}} = \epsilon_\omega \sigma T_\omega^4 + (1-\epsilon_\omega)\sigma\theta_{\mathrm{R}}^4(0) + \frac{\epsilon_\omega - 3}{2} q_{\mathrm{n}}(0) \qquad (20)$$

When $\epsilon_\omega = 1$, then Equations (19) and (20) are equivalent and $\theta_{\mathrm{R}}^4(0)$ cannot formally be determined. From the continuity requirement $\theta_{\mathrm{R}}|_{\epsilon_\omega=1} = \theta_{\mathrm{R}}|_{\epsilon_\omega\to 1}$, however, we can treat Equation (20) for $\epsilon_\omega = 1$ as that for $\epsilon_\omega \to 1$. In this case, eliminating q_{inc} from Equations (19) and (20), the following equation is obtained:

$$q_{\mathrm{n}}(0) = \frac{\sigma(T_\omega^4 - \theta_{\mathrm{R}}^4)}{\left(\dfrac{1}{\epsilon_\omega} - \dfrac{1}{2}\right)} \qquad (21)$$

The thermal radiation transfer problem in the P-1 model effectively reduces to the solution of Equation (18), with the boundary condition (21), which is linked to the enthalpy equation via the term $-\nabla q$ determined by Equation (17). This means that instead of the distribution of the radiation intensity along the set of rays, only the spatial distribution of the scalar parameter θ_{R} needs to be computed. This makes the P-1 model particularly attractive for implementation in conventional computational fluid dynamics (CFD) packages, especially those using body fitted coordinates (FLUENT is one of these packages). The effects of scattering are accounted for in the P-1 model at no extra computer time cost.

The main disadvantage of the P-1 model is that its accuracy cannot easily be improved by increasing the number of terms in Equation (3). This means that the reliability of the P-1 model for modelling realistic thermal radiation processes can in general be established mainly by trial and error rather than rigorous analysis. Nevertheless it appears to be possible to make qualitative predictions about the reliability of the P-1 model for particular geometries without time-consuming and expensive testing, as will be shown below.

LIMITATIONS

The main assumption of the P-1 model is that the function $i'(s, \theta, \varphi)$ can be presented in the form (6). In the case of an axisymmteric problem when $i'(s, \theta, \varphi) = i'(s, \theta)$ (does not depend on φ), Equation (6) can be simplified to

$$i' = a(\boldsymbol{s}) + b(\boldsymbol{s})\cos\theta \qquad (22)$$

where the coefficients $a(\boldsymbol{s}) = i'^{(0)}/4\pi$ and $b(\boldsymbol{s}) = 3i'^{(1)}/4\pi$ are functions of the radius vector $\boldsymbol{s}$.

In the case of a 1D plane geometry (radiation exchange between two infinite parallel planes with participating medium between them) the physical meaning of coefficients $a(\boldsymbol{s})$ and $b(\boldsymbol{s})$ is straightforward: $a(\boldsymbol{s})$ accounts for the volumetric radiation from the medium (which is independent of θ), while $b(\boldsymbol{s})$ accounts for the radiation from the points on the stratified layers (boundaries) to a given point, which is proportional to $\cos\theta$. This follows from the fact that the intensity of radiation recorded at the point A (see *Figure 1*) is

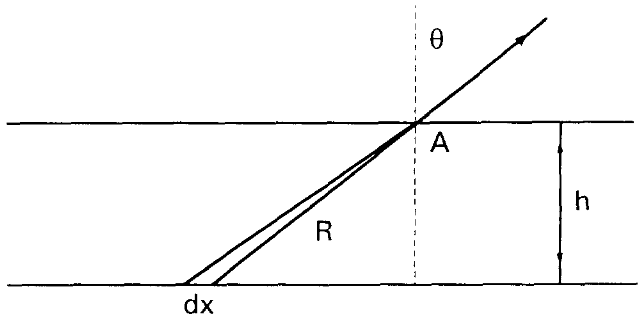

Figure 1 Schematic presentation of the process of radiation transfer between two parallel planes in an optically thin medium

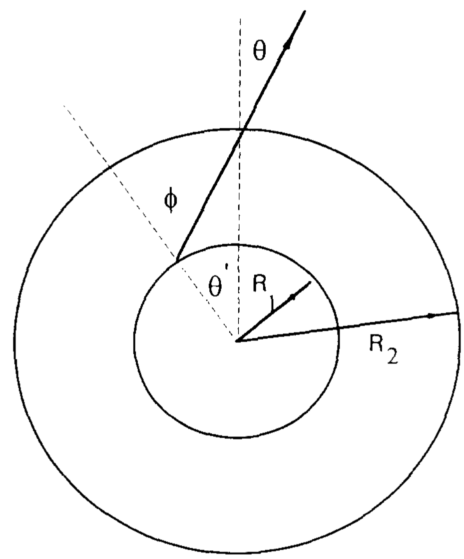

Figure 2 Schematic presentation of the process of radiation transfer between two concentric spheres in an optically thin medium

proportional to $1/R^2$ and the area of the emitting element of the surface dx, which in turn is proportional to R, where R is the distance from the emitting element of the surface dx; $R = h/\cos\theta$, where h is the shortest distance between the point A and the plane under consideration. Note that the intensity of the radiation emitted from the plane does not depend on θ. In this case the presentation (22) is exact, as it accounts for all possible sources of radiation in the problem under consideration. Hence it can be expected that this problem can be solved accurately based on the P-1 model. This conclusion is consistent with the result reported in ref. 6, where it was shown that the radiation heat fluxes in this geometry predicted by the P-1 and P-3 models are indistinguishable within the accuracy of plotting. Presentation (22) seems to have a clear advantage over the two-flux model[1] (in which it is assumed that $i' =$ const. over a given range of θ, say for positive and negative θ), at least for the plane geometry.

However, the situation appears to be different if localized sources of heat are present in the system. Consider for example the problem of heat exchange between concentric spheres of radii R_1 and R_2 ($R_1 < R_2$) at temperatures T_1 and T_2 with absorbing and radiating medium between them. First consider the limiting case of transparent gas, so that the problem can be reduced to radiative exchange between these two spheres. Owing to the symmetry of the problem, the P-1 model approximation for i' reduces to Equation (22).

One of the rays leaving the inner sphere and reaching the outer sphere at the angle θ is shown in *Figure 2*. This ray leaves the inner sphere at the angle $\phi = \theta + \theta'$. The maximal value of $\phi = \pi/2$ is attained at

$$\theta = \theta_{\max} = \arcsin(R_1/R_2) < \pi/2 \tag{23}$$

Condition (23) means that $i(\theta > \theta_{\max}) = 0$, which contradicts the initial assumption (22). In other words, if Equation (22) is used with $a(s) = 0$ and $b(s)$ providing the correct result for $\theta = 0$, then an extra spurious radiative flux accounted for Equation (22) at $\theta > \theta_{\max}$ can arise. The radiative flux accounted for by the P-1 model can be estimated as

$$q_{\mathrm{p1}} = b(s)\int_0^{\pi/2} \cos^2\theta \,\mathrm{d}\theta = \pi b(s)/4 = 0.785b(s) \tag{24}$$

while the actual radiative flux is defined by the expression

$$q_{\mathrm{actual}} = b(s)\int_0^{\theta_{\max}} \cos(\theta+\theta')\cos\theta \,\mathrm{d}\theta \tag{25}$$

where

$$\theta = \arctan\left[\frac{R_1 \sin\theta'}{R_2 - R_1\cos\theta'}\right] \tag{26}$$

Consider the particular case $R_2 = 2R_1$, when Equation (26) reduces to (remembering that the main contribution to the integral in Equation (25) comes from small values of θ')

$$\theta \approx \theta' \tag{27}$$

Note that the approximation (27) can be poor when R_2 is not close to $2R_1$. In this case the general formula (26) needs to be used.

Substituting Equation (27) into Equation (25) gives (remembering that $\theta_{\max}$ in this case is equal to $\pi/4$)

$$q_{\mathrm{actual}} = b(s)\int_0^{\pi/4} \cos(2\theta)\cos\theta \,\mathrm{d}\theta$$

$$= b(s)\left[\sin\theta - \frac{2\sin^3\theta}{3}\right]_0^{\pi/4} = 0.471b(s) \tag{28}$$

From Equations (24) and (28) it is found that $q_{\mathrm{p1}}/q_{\mathrm{actual}} = 1.67$. This agrees well with what is predicted by the rigorous analysis (cf. Figure 15–11 of ref. 1, which predicts $q_{\mathrm{p1}}/q_{\mathrm{actual}} = 1.66$ for zero optical thickness).

For optically thick media, only the layers in the immediate vicinity of the point under consideration need to be accounted for. These layers can be treated as planes, which justifies the presentation (22).

Although the simplistic analysis described in this section cannot be used for quantitative prediction of the radiation transfer, it allows some useful rough estimates of the limitations of the P-1 model. That is, for plane geometries this model seems to be applicable both for optically thick and optically thin media. However, caution is needed when the model is applied to optically thin enclosures with localized sources of heat. (This is consistent with the results of computations presented in ref. 1: see Figures 15–10 and 15–11 therein.)

INTERACTION OF RADIATION WITH PARTICLES

If particles are present in a combustion chamber, then Equation (2) can be generalized[7] to

$$\frac{\mathrm{d}i'}{\mathrm{d}s} = a(i'_{\mathrm{b}} - i') - \sum_n \left[(\epsilon_{\mathrm{p}} + r_{\mathrm{p}})A_{\mathrm{p}n}i' + \epsilon_{\mathrm{p}}A_{\mathrm{p}n}i_{\mathrm{p}n} + \frac{r_{\mathrm{p}}A_{\mathrm{p}n}}{4\pi}\int_{\omega_i=0}^{4\pi} i'(s,\omega_i)P(\omega,\omega_i)\,\mathrm{d}\omega_i\right] \tag{29}$$

where ϵ_{p} is the particles' emissivity (equal to absorptivity), r_{p} is their reflectivity (both are assumed to be the same for all particles), $A_{\mathrm{p}n}$ is the projected area of the nth particle per unit volume and $P(\omega, \omega_i)$ has the same meaning as $\Phi(\lambda, \omega, \omega_i)$ in Equation (1) but refers to particle scattering, and i_{p} has the same meaning as i_{b} but refers to particles. In deriving Equation (29) it was assumed that particles are the only scattering component in the system. The summation is assumed over all particles in unit volume.

Assuming that $P(\omega, \omega_i) = f = \text{const.}$, and the P-1 model approximations, Equation (29) can be reduced to

$$\frac{1}{3}\nabla\frac{1}{a_\Sigma}\nabla\theta_{\mathrm{R}}^4 - a(\theta_{\mathrm{R}}^4 - T^4) + \epsilon_{\mathrm{p}}\sum_n[A_{\mathrm{p}n}(T_{\mathrm{p}n}^4 - \theta_{\mathrm{R}}^4)] = 0 \tag{30}$$

where

$$a_\Sigma = a + \sum_n A_{\mathrm{p}n}[\epsilon_{\mathrm{p}} + r_{\mathrm{p}}(1-f)] \tag{31}$$

and T_{p} is the temperature of the particles and f the scattering factor. Other notation is the same as in Equation (18).

Equation (30) can be solved similarly to Equation (18) with the formal replacements

$$\left.\begin{aligned} a + \sigma_{\mathrm{s}} &\to a_\Sigma \\ 3a &\to 3\left(a + \epsilon_{\mathrm{p}}\sum_n A_{\mathrm{p}n}\right) \\ aT^4 &\to aT^4 + \epsilon_{\mathrm{p}}\sum_n A_{\mathrm{p}n}T_{\mathrm{p}n}^4 \end{aligned}\right\} \tag{32}$$

The boundary condition for Equation (30) is the same as for Equation (18).

APPLICATION TO COAL COMBUSTION MODELLING

In the real industrial environment, modelling of the effects of thermal radiation is performed in connection with the modelling of a number of other effects including turbulence, combustion processes, coal devolatilization and heterogeneous char reaction. Modelling of all these processes requires a large number of specific assumptions, the applicability of which is not at first evident. A common way of justifying these assumptions is based on comparison of the results of modelling with available experimental data. Although this comparison may not always be conclusive, owing to the large number of the processes involved, it usually provides a useful indication of the reliability or otherwise of the models.

This section compares the temperatures observed inside a $2\,MW_t$ furnace (IFRF MMF5-2) and those predicted by the modelling of the coal combustion processes based on the FLUENT software package. Two models of radiation transfer are implemented in this package: a discrete transfer radiation model and the P-1 model. The latter model is particularly convenient for modelling of coal combustion processes, as it describes in the most convenient way the radiation exchange between gas and coal particles (see above). This model has been used for the present analysis.

The scheme of the furnace is shown in *Figure 3*. Combustion air and pulverized fuel (coal) enter the furnace through a single swirl stabilized burner. The swirl number for the combustion air is 0.92 and the burner operates in the conventional unstaged fashion. The coal fired is Gottelbern high-volatile bituminous, with a mean particle size of 45 μm. Extensive data for this

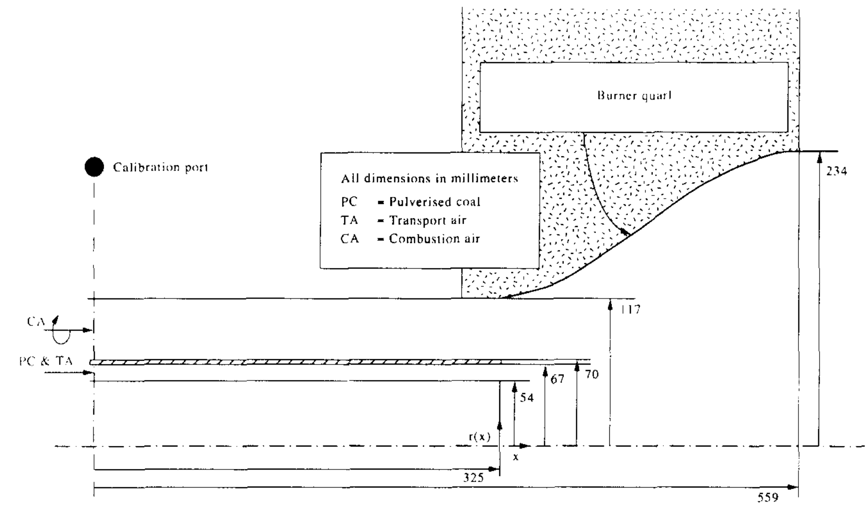

Figure 3 General scheme of burner geometry

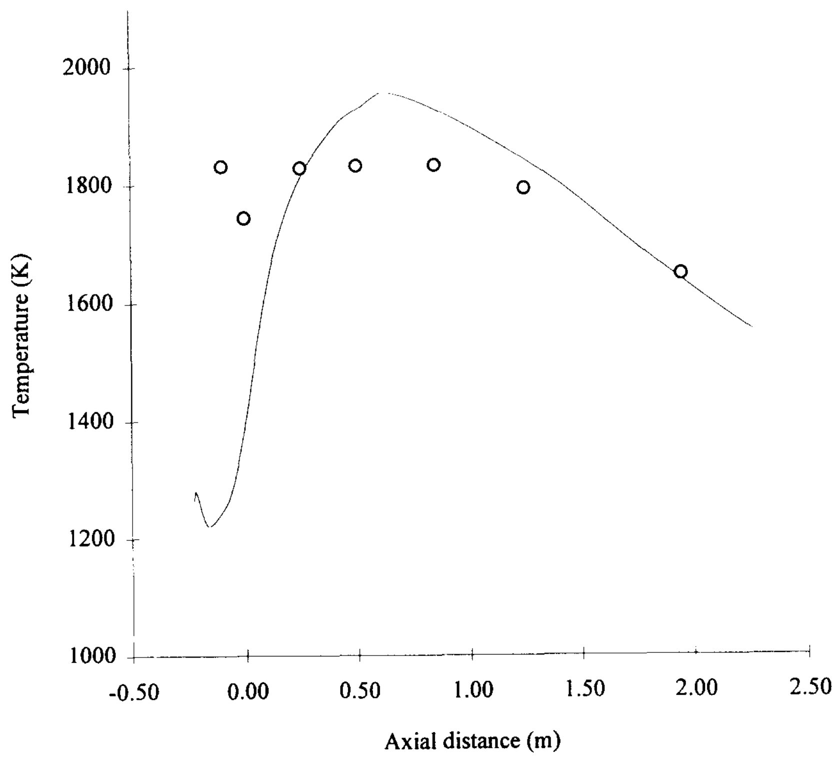

Figure 4 Experimental (○) and predicted (—) axial profiles of temperature. The point $x = 0$ corresponds to the point at 559 mm from the inlet (see *Figure 3*)

flame together with all operating parameters are documented in ref. 8. The system has been modelled using a two-dimensional axisymmetric grid of 191×121 computational cells. This allows the burner to be modelled in detail but with the furnace geometry approximated to that of a cylinder.

Details of the results of the modelling and the approximations used will be described elsewhere. Here only measured and predicted temperature profiles at the burner axis are presented: *Figure 4*. As can be seen, peak temperatures at the axis are only slightly overpredicted. The coincidence of measured and predicted downstream temperatures is almost ideal. Inside quarl temperatures however are underpredicted significantly (by $\sim 30\%$). This underprediction could be explained by the fact that the modelled coal devolatilization and combustion rates fail to predict the fast heat release in this region.

CONCLUSIONS

In the case of plane 1D geometry the P-1 model is expected to make reliable predictions in both optically thick and optically thin media. A combination of simplicity and reliability makes the P-1 model particularly attractive for the modelling of processes of thermal radiation transfer in industrial environments, except when the radiation effects from localized heat sources in optically thin media need to be accurately accounted for. Another advantage of the P-1 model is that it allows the radiation exchange with particles to be accounted for in a relatively simple way. Computations of the distribution of temperatures inside a coal furnace based on the P-1 model are in reasonably good agreement with the results of direct measurements.

ACKNOWLEDGEMENTS

The authors are grateful to H. F. Boysan for useful discussion of the problems considered in this paper.

REFERENCES

1 Siegel, R. and Howell, J. R. 'Thermal Radiation Heat Transfer', Hemisphere Publishing Corporation, Washington, DC, 1992
2 Viskanta, R. and Mengüc, M. P. *Prog. Energy Combust. Sci.* 1987, **13,** 97
3 Pomraning, G. C. and Foglesong, G. M. *J. Comput. Phys.* 1979, **32,** 420
4 Arscott, J. A., Gibb, J. and Jenner, R. In 'Combustion Institute European Symposium' (Ed. F. J. Weinberg), Sheffield, 1973, 674
5 Marshak, R. E. *Phys. Rev.* 1947, **71,** 443
6 Bayazitoglu, Y. and Higenyi, J. *AIAA J.* 1979, **17,** 424
7 Lockwood, F. C., Rizvi, S. M. A. and Shah, N. G. *Proc. Inst. Mech. Eng.* 1986, **200,** 79 (Also in Eighteenth Symposium (International) on Combustion', The Combustion Institute, Pittsburgh, 1981)
8 Peters, A. A. F. and Weber, R. 'Modelling of swirling natural gas and pulverized coal flames with emphasis on nitrogen oxides', IFRF Doc. No. F 36/Y/21D, International Flame Research Foundation, IJmuiden, 1993